

Theory of small-angle neutron scattering from the imperfect vortex lattice in type-II superconductors

E. H. Brandt*

Ames Laboratory—United States Department of Energy and Department of Physics, Iowa State University, Ames, Iowa 50011

(Received 19 June 1978)

A theory of the neutron scattering intensity from an imperfect vortex lattice in type-II superconductors is developed, which predicts that flux pinning leads not only to a broadening of the Bragg reflections, but also to a finite scattering intensity for wave vectors within the first Brillouin zone. At sufficiently high fields, the small-angle scattering intensity is predicted to exceed that of the Bragg reflections. According to this theory, if the incident beam is chosen parallel to the applied field, shear and tilt strains in the vortex lattice, and thus the most important intrinsic defects, give no contribution to small-angle scattering, and the measured intensity is due almost entirely to the strains caused by pinning forces. Small-angle neutron scattering experiments are thus capable of yielding insight into elementary pinning interactions beyond that obtainable from volume pinning force measurements, which must be interpreted by means of still unsatisfactory statistical summation theories.

I. INTRODUCTION

The magnetic field inside a type-II superconductor to which an external field $H_a > H_{c1}$ is applied exhibits spatial variations due to the appearance of flux lines, which form a flux-line lattice (FLL). If a beam of monochromatic neutrons is applied to the specimen, some of the neutrons are scattered by a small angle, the scattering amplitude being proportional to the Fourier transform of the internal field $\vec{H}(\vec{r})$. Neutron scattering has been used to determine the symmetry and spacing of the FLL, the field distribution within a lattice cell, and the curvature of flux lines.¹⁻¹⁴

In a real superconductor the pinning forces exerted on the flux lines by crystal imperfections distort the FLL and smear out the Bragg reflections of the ideal FLL. As recently pointed out by Labusch,¹⁵ the intensity profile of the diffraction lines gives insight into properties of the pinning forces. This theory predicts not only a weakening of the sharp lines by Debye-Waller factors, but also the appearance of a broadened profile, whose width gives a measure of the mean square of the pinning forces. Neutron scattering thus complements measurements of critical currents, flux density gradients, and irreversible magnetization curves, which all determine the maximum volume-pinning force of the imperfect matrix on the FLL. As for the elementary pinning forces, there is at present no method that determines the forces exerted on each flux line within a FLL without the aid of statistical summation theories. The existing summation theories¹⁶⁻¹⁹ are restricted to the so-called dilute limit, and in the three-dimensional case yield a threshold for

the elementary pinning force below which the volume pinning force should vanish. There is no experimental evidence for this threshold.

It is therefore desirable to get further information on flux pinning. This is particularly important at high inductions, $b = B/B_{c2} > 0.3$, where the flux line cores overlap, even if the Ginsburg-Landau (GL) parameter κ is large. This overlap invalidates the usual picture of individual flux lines interacting with each other and with the pinning centers by two-body interactions. This picture underlies all existing quantitative theories on flux pinning. In those theories the only two corrections adopted from the GL theory are that the pinning forces and the shear modulus of the FLL are allowed to vanish as $b \rightarrow 1$. As shown recently,²⁰⁻²⁷ a rigorous GL treatment of the pinning problem yields the fact that both the elastic properties of the FLL and the character of pinning forces require further modifications at large inductions. These modifications are used in this paper.

The method in which information about pinning forces is extracted from the shape of diffraction lines has several drawbacks that are most severe just at large inductions where this information is most desirable. One disadvantage is the low intensity of even the most intense reflection. Since the spatial variations of the magnetic field are of order $H_{c2}(1-b)/\kappa^2$ (ideal FLL at $b > 1/2\kappa^2$), the scattered intensity behaves as $(1-b)^2/\kappa^4$ and thus is low for large values of b and κ . This estimate also shows that, without pinning, the field inside a hard superconductor ($\kappa \gg 1$) is practically constant, except at very low inductions $b < 1/2\kappa^2$. It is therefore difficult to measure the line profile at large inductions or in hard superconductors.

The sharp lines predicted by Ref. 15 appear only if the flux line displacements from a perfect reference lattice are small compared with the lattice spacing d . For a specimen of diameter D this means that the relative deviations of the induction from its spatial average should not exceed the value $0.1d/D$, which is typically of order 10^{-5} . Such a high homogeneity probably cannot be achieved in macroscopic specimens. This is true particularly at large inductions, since the stiffness of the FLL decreases more rapidly with the induction than do the pinning forces.

There is also an objection of a more fundamental nature. For the calculation of the intensity profile it was postulated that the scattering cross section splits up into the product of a structure factor and a form factor, which is assumed to be insensitive to lattice distortions. This assumption implies that the magnetic field is the linear superposition of effective vortex fields, each of which is centered at one flux line, or if bending of flux lines is allowed for, at one flux line element. However, at large inductions, and for κ close to $1/\sqrt{2}$ even at arbitrary induction, this assumption probably does not apply even approximately. In these two special cases the magnetic field is related to the order parameter $\omega(\vec{r}) = |\Psi(\vec{r})|^2$ and to the applied field H_a by the local relationship $H(\vec{r}) = H_a - H_{c2}\omega(\vec{r})/2\kappa^2$. The order parameter of the distorted FLL takes the form of a product (which ensures $\omega = 0$ at the flux line centers) rather than a sum.²² It is not yet clear to us in which cases the product may be approximated by a sum, thus ensuring the form factors to be independent of the lattice distortions. The interpretation of the intensity profile requires a detailed calculation of the rapidly varying part of the magnetic field of the distorted FLL. At present, only the slowly varying part is known with sufficient accuracy.^{22,23}

We therefore suggest experiments measuring the intensity of neutrons with scattering vector inside the first Brillouin zone (BZ) of the FLL rather than close to the reciprocal-lattice vectors. It will be shown that this small-angle-scattering method yields detailed information on the lattice distortions and on the pinning forces. The method will avoid most of the disadvantages of the line-profile method: (i) The scattered intensity will be large at large inductions and a modest angular resolution or even integral measurements will suffice, (ii) small displacements are not postulated, and, most importantly, (iii) the theory is based entirely on the GL equations and thus avoids the *ad hoc* assumptions of displacement-independent form factors, local-elasticity theory, and local pinning forces which were used in Ref. 15.

II. SCATTERING FROM STRAINS IN THE FLUX-LINE LATTICE

The differential scattering cross section for neutrons within the Born approximation²⁸ is

$$\frac{d\sigma}{d\Omega} = \left(\frac{\mu_0 \gamma_n}{4\phi_0} \right)^2 |\vec{H}(\vec{k})|^2 = I(\vec{k}) \quad (2.1)$$

(in Système International units), where $\gamma_n = 1.91$, ϕ_0 is the quantum of flux, k is the scattering vector, and $\vec{H}(\vec{k})$ is the Fourier transform of the magnetic field inside the superconductor defined by

$$\vec{H}(\vec{r}) = \int \frac{d^3k}{8\pi^3} e^{i\vec{k}\cdot\vec{r}} \vec{H}(\vec{k}), \quad (2.2a)$$

$$\vec{H}(\vec{k}) = \int_V d^3r e^{-i\vec{k}\cdot\vec{r}} \vec{H}(\vec{r}). \quad (2.2b)$$

The spatial integration in (2.2b) extends over the volume V of the specimen. $\vec{H}(\vec{r})$ is completely determined, at least in principle, by the boundary conditions, by the positions of the flux lines, and by the material parameters and temperature entering the theory chosen.

In the following we need the discrete fields $s_\nu(z) = (s_{\nu,x}(z), s_{\nu,y}(z), 0)$, the displacement of the ν th flux line measured in the plane $z = \text{const}$ from the regular flux-line position $\vec{R}_\nu = (X_\nu, Y_\nu, z)$, and $\vec{P}_\nu(z) = (P_{\nu,x}(z), P_{\nu,y}(z), 0)$, the pinning-force density. These fields are discrete with respect to the variable ν (indicating the flux line) and continuous with respect to z (a line parameter, for which we choose the coordinate z parallel to the applied field). The Fourier transforms of $\vec{s}_\nu(z)$ and $\vec{P}_\nu(z)$ are continuous functions $\vec{s}(\vec{k})$ and $\vec{P}(\vec{k})$ defined, e.g., by

$$\vec{P}_\nu(z) = \int_{\text{BZ}} \frac{d^3k}{8\pi^3 n} e^{i\vec{k}\cdot\vec{R}_\nu} \vec{P}(\vec{k}), \quad (2.3a)$$

$$\vec{P}(\vec{k}) = \sum_\nu \int dz e^{-i\vec{k}\cdot\vec{R}_\nu} \vec{P}_\nu(z). \quad (2.3b)$$

In (2.3a) $n = B/\phi_0$ is the average density of flux lines and the integration is over the BZ. From (2.3b) it follows that $\vec{s}(\vec{k})$ and $\vec{P}(\vec{k})$ are periodic in \vec{k} . In contrast to this, the integration in (2.2a) extends to infinity and $\vec{H}(\vec{k})$ is not periodic. For an ideal periodic FLL one has

$$\vec{H}(\vec{r}) = \sum_{\vec{K}} \vec{H}_{\vec{K}} e^{i\vec{K}\cdot\vec{r}}, \quad (2.4a)$$

$$\vec{H}(\vec{k}) = \sum_{\vec{K}} \vec{H}_{\vec{K}} 8\pi^3 \delta(\vec{k} - \vec{K}), \quad (2.4b)$$

where the δ function is $\delta(k_x - K_x) \delta(k_y - K_y) \delta(k_z)$, and the sum is over all reciprocal-lattice vectors $\vec{K} = (K_x, K_y, 0)$. Due to the factor $\delta(k_z)$, the scat-

tering intensity of the ideal lattice vanishes outside the plane $k_z = 0$. This is shown in Fig. 1.

For an imperfect FLL $\vec{H}(\vec{r})$ is no longer strictly periodic and the δ functions in (2.4b) will be smeared out. In addition to this, long-wavelength variations of $\vec{H}(\vec{r})$, with wave vectors \vec{k} within the first BZ, will occur and lead to a finite scattering amplitude at small scattering wave vectors (Fig. 2). For such small \vec{k} the GL theory yields²³

$$\vec{H}(\vec{k}) = \frac{\phi_0}{\mu_0} \frac{-\hat{z} [i\vec{k} \cdot \vec{s}(\vec{k})] + ik_z \vec{s}(\vec{k})}{1 + k^2/k_h^2} \quad (2.5)$$

plus terms of higher order in the strains and in k^2/K_{10}^2 (\vec{K}_{10} is the first reciprocal-lattice vector). Equation (2.5) applies to all values of κ and b and to wave vectors $k \leq 0.7 k_B$, where k_B is the radius of the BZ. The three characteristic wave vectors appearing here and in the following are

$$k_B^2 = 2b/\xi^2 = 4\pi n, \quad (2.6)$$

$$k_h^2 = \langle \omega \rangle / \lambda^2 \approx [(1-b)/2b\kappa^2] k_B^2, \quad (2.7)$$

$$k_\psi^2 = 2(1-b)/\xi^2 = [(1-b)/b] k_B^2, \quad (2.8)$$

where λ is the weak-field penetration depth, $\xi = \lambda/\kappa$, and $\langle \omega \rangle \approx 1-b$ is the spatial average of the order parameter. For the triangular FLL, $K_{10}^2 = (2\pi/\sqrt{3})k_B^2$, or $k_B = 1.05 (\frac{1}{2}K_{10})$.

Equation (2.5) states that for periodic displacement fields the z component of $\vec{H}(\vec{r})$ varies spatially with the amplitude $-B \text{div} \vec{s}(\vec{r}) (1+k^2/k_h^2)^{-1}$, where $-\text{div} \vec{s}(\vec{r})$ is the local compression of the FLL. In addition to this, a field component $B(\partial/\partial z) \vec{s}(\vec{r}) (1+k^2/k_h^2)^{-1}$ appears that is proportional to the local tilting angle of the flux lines and directed perpendicular to z ; this component ensures that $\text{div} \vec{H}(\vec{r}) = 0$. The factor $(1+k^2/k_h^2)^{-1}$

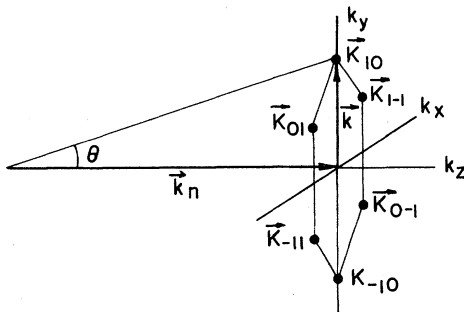


FIG. 1. Schematic representation of the scattering geometry for incident neutron beam and applied field \vec{H}_a parallel to the z axis for an ideal hexagonal FLL. The scattering intensity is finite only at the reciprocal-lattice points $\vec{K}_{mn} = \vec{k}$. The neutron wave vector \vec{k}_n and the scattering angle θ are not drawn to scale; for $2\pi/k_n = 4 \text{ \AA}$ and $B = 1000 \text{ G}$, $\theta = 0.0016 \text{ rad}$. The total intensity of each reflection has to be measured by rocking the sample.

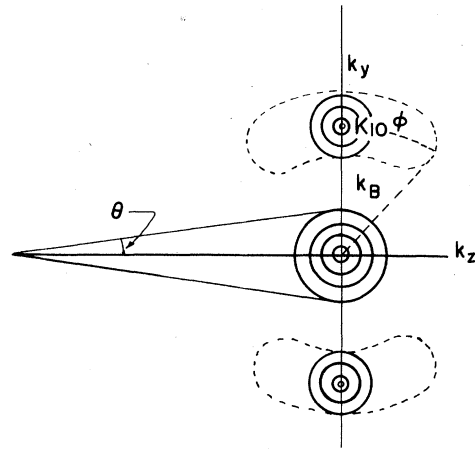


FIG. 2. Lines of constant scattering intensity for a perturbed FLL (schematic). If the FLL is a polycrystal, the intensity distribution is rotationally symmetric about the k_z axis (which is parallel to \vec{H}_a). The planes of constant intensity are tori of elliptical cross section and with radii K_{mn} and ellipsoids centered at the origin. These ellipsoids are calculated in this paper. The smearing out of the Bragg reflections by rocking the sample is indicated by a dashed line.

may be interpreted as originating from the overlap of effective vortex fields having a range k_h^{-1} . Indeed, Eq. (2.5) coincides with the corresponding result of the London theory²³ with λ replaced by k_h^{-1} . This coincidence is, however, restricted to $k < 0.7 k_B$. At larger k the GL result for the field of the distorted FLL only approximately coincides with a linear superposition of effective vortex fields, the deviation being largest at large values of b and k .

Inserting (2.5) into (2.1), we get a basic formula for the differential scattering cross section of the distorted FLL:

$$I(\vec{k}) = \left(\frac{1.91}{4} \right)^2 \frac{|\vec{k} \cdot \vec{s}(\vec{k})|^2 + k_z^2 |\vec{s}(\vec{k})|^2}{(1 + k^2/k_h^2)^2}. \quad (2.9)$$

III. SCATTERING DUE TO PINNING FORCES

Distortions of the FLL may be caused by intrinsic defects or by pinning forces. Within linear theory of elasticity, the most important intrinsic defects (edge and screw dislocations and point defects²⁹) cause mere shear or tilting strains. Both intrinsic strain types satisfy the condition $\text{div} \vec{s} = \vec{k}\vec{s} = 0$: for the shear strain $\text{div} \vec{s}$ vanishes by definition, and for screw dislocations it vanishes because \vec{s} depends only on z but has no z component. Thus the first term in (2.9) vanishes identically for intrinsic strains. The second term can be made extremely small by choosing the incident beam parallel to the external field.

In this geometry the scattering vector for elastic scattering has a negligibly small z component, since for thermal neutrons the wave vector k_n is much larger than the scattering vector k .

We now express the displacements that appear in the scattering intensity (2.9) in terms of the pinning forces. The most general linear relationship between these fields takes a simple form if expressed in Fourier space,

$$\vec{s}(\vec{k}) = \vec{\phi}^{-1}(\vec{k}) \vec{P}(\vec{k}), \quad (3.1)$$

where $\vec{\phi}^{-1}(\vec{k})$ is the inverse of the elastic matrix $\vec{\phi}(\vec{k})$ of the FLL. Within the continuum approximation,^{24,26} which is valid for $k \lesssim 0.7 k_B$, the GL theory yields an expression for $\vec{\phi}(\vec{k})$ that is similar to that of the local theory of elasticity but with the elastic moduli replaced by \vec{k} -dependent functions:

$$\vec{\phi}(\vec{k}) = \frac{1}{n} \begin{pmatrix} c_{11}(k)k_x^2 + c_{66}k_y^2 + c_{44}(k)k_z^2 + \alpha_L; & [c_{11}(k) - c_{66}]k_x k_y \\ [c_{11}(k) - c_{66}]k_x k_y; & c_{11}(k)k_y^2 + c_{66}k_x^2 + c_{44}(k)k_z^2 + \alpha_L \end{pmatrix}, \quad (3.2)$$

with

$$c_{11}(k) = (B^2 dH_a/dB)/(1 + k^2/k_n^2)(1 + k^2/k_y^2), \quad (3.3)$$

$$c_{66} \approx BH_{c2}[(1-b)^2/10\kappa^2](1 - 1/2\kappa^2), \quad (3.4)$$

$$c_{44}(k) = (B^2/\mu_0)/(1 + k^2/k_n^2) + B(H_a - B/\mu_0). \quad (3.5)$$

The parameter α_L , first introduced by Labusch,³⁰ emerges from the statistics of pinning centers (cf. Sec. IV). It removes a divergence of the scattering amplitude at small scattering angles.

Inserting (3.1) into (2.9), we get for longitudinal geometry (beam parallel to z)

$$I(k_x, k_y, 0) = 0.23 \frac{n^2}{(1 + k^2/k_n^2)^2} \frac{|\vec{k} \cdot \vec{P}(k_x, k_y, 0)|^2}{[c_{11}(k)k_x^2 + \alpha_L]^2}, \quad (3.6)$$

and for transversal geometry (beam perpendicular to z),

$$I(k_x, 0, k_z) = 0.23 \frac{n^2}{(1 + k^2/k_n^2)^2} \left(\frac{|\vec{P}_x(k_x, 0, k_z)|^2(k_x^2 + k_z^2)}{[c_{11}(k)k_x^2 + c_{44}(k)k_z^2 + \alpha_L]^2} + \frac{|\vec{P}_y(k_x, 0, k_z)|^2 k_z^2}{[c_{66}k_x^2 + c_{44}(k)k_z^2 + \alpha_L]^2} + \frac{k_z^2}{n^2} |\vec{s}_{in}(\vec{k})|^2 \right). \quad (3.7)$$

In (3.7) appear the displacements caused by intrinsic defects, $\vec{s}_{in}(\vec{k})$, which were assumed to be uncorrelated with the displacements caused by pinning forces. For longitudinal geometry this assumption is not required. For cases where rotational symmetry about the z axis applies, the general result $I(k_x, k_y, k_z)$ is obtained from (3.7) by replacing k_x^2 with $k_x^2 + k_y^2$. The two expressions (3.6) and (3.7) still apply to the general case where this symmetry does not exist, for instance, because of a transport current or asymmetric flux density gradient. By measuring at various orientations between the incident neutron beam and the transport current, one would get additional information about the distribution of pinning forces.

IV. STATISTICS OF PINNING FORCES

The squares $|\vec{e} \cdot \vec{P}(\vec{k})|^2$ appearing in (3.6) and (3.7) with $\vec{e} = \vec{k}$, \vec{x} , or \vec{y} can be calculated from the force field of individual pinning centers. First consider a superconductor containing a large number of pinning centers of various types with positions distributed at random. From (2.3b) it follows that the $\vec{P}(\vec{k})$ of two pinning centers of the

same type and at equivalent positions (differing by a lattice vector \vec{R}_v) differ only by a phase factor $\exp(-i\vec{k} \cdot \vec{R}_v)$. If there are many pinning centers of that type at equivalent positions, then in the square of the sum over all force fields the cross terms give no contribution because of destructive interference of the phase factors, and one is left with

$$|\vec{e} \cdot \vec{P}(\vec{k})|^2 = \left| \sum_i \vec{e} \cdot \vec{P}_i(\vec{k}) \right|^2 = \sum_i |\vec{e} \cdot \vec{P}_i(\vec{k})|^2, \quad (4.1)$$

where $\vec{P}_i(\vec{k}, \vec{a})$ is the force field of a pinning center situated at $\vec{r} = \vec{a}$ and the average is over all possible positions \vec{a} . If the \vec{a} are at random, one should hope to obtain this average by averaging over homogeneously distributed positions \vec{a} within one lattice cell. This is indeed true if one deals with forces on a rigid lattice. Elasticity of the FLL introduces, however, two complications.

First, the pinning forces are not completely independent of each other since the flux line displacements caused by one pinning center change the distance between the flux lines and the pinning centers, thereby changing also the original stiff-

lattice pinning forces. This effect is approximately taken into account by Labusch's parameter α_L in the elastic matrix (3.2). This parameter adds to the elastic interaction between the flux lines an elastic interaction between each flux line element and its original position in the ideal FLL. This approximation makes sense only for sufficiently weak pinning interactions and for wave vectors \vec{k} much smaller than the reciprocal mean distance between pinning centers. It is, therefore, consistent to keep α_L in (3.6) and (3.7) only in order to prevent the divergence as $k \rightarrow 0$, but neglect all combinations of α_L with k_h^2 and k_ψ^2 when (3.3) and (3.4) are inserted.³¹

Second, if we calculate the pinning-force field from the interaction with the unperturbed FLL, as will be done below, we get too large a value for $|\vec{e} \cdot \vec{P}(\vec{k})|^2$, since the elastic response of the FLL tends to reduce the pinning forces. This effect will lead to a breakdown of the following calculations at inductions close to B_{c2} , where finally all flux lines are trapped by pinning centers and the displacements cannot increase further. This saturation may be approximately accounted for by performing the average (16) over the lattice cell with a weight factor $g(\vec{a})$ that favors the center of the lattice cell for attractive pinning forces and the cell boundary for repulsive forces (if the cell is centered at a flux line). In this paper the averages will be evaluated for $g(\vec{a}) = 1$, which means that the lattice distortions are assumed to be small.

Putting these arguments together and specializing to longitudinal geometry (to which the following sections are restricted), we arrive at the differential scattering cross section

$$I(k_x, k_y, 0) = 0.23 \frac{n^2(1 + k^2/k_\psi^2)^2}{[c_{11}(0)k^2 + \alpha_L]^2} \times N \langle |\vec{k} \cdot \vec{P}(k_x, k_y, 0; \vec{a})|^2 g(\vec{a}) \rangle, \quad (4.2)$$

where the average is taken over the unit cell of the FLL and $\langle g(\vec{a}) \rangle = 1$. Note that the factor $(1 + k^2/k_h^2)$ in the compressional modulus (3.3) and in the field (2.6) have canceled, and the final result (4.2) contains the usual compressional modulus $c_{11}(0) = c_{11}$ of the local elasticity theory. The nonlocal elastic response of the FLL leads to the appearance of the factor $(1 + k^2/k_\psi^2)$ in the scattered intensity. This factor may be neglected at $b < 0.5$; at larger inductions it leads, however, to the quite unexpected result of a b -independent scattering intensity. This will be shown in the following sections for point pinning centers.

V. SIMPLE-PINNING-FORCE MODELS

If each pinning center acts on one flux line only, the average in (4.3) is easily evaluated. For a pinning center acting with a force \vec{P}_i on the flux line situated at $\vec{R}_{\nu,i}$, Eq. (2.3b) gives $\vec{P}(k_x, k_y, 0) = \vec{P}_i \exp(-i\vec{k} \cdot \vec{R}_{\nu,i})$. This result is independent of the detailed behavior of the force density along this flux line. For many uncorrelated pinning centers one gets

$$|\vec{k} \cdot \vec{P}(k_x, k_y, 0)|^2 = k_x^2 \sum_i P_{x,i}^2 + k_y^2 \sum_i P_{y,i}^2. \quad (5.1)$$

If the force distribution is isotropic (no transport current), the two sums in (5.1) are equal. The scattering intensity (4.3) then becomes

$$I(k_x, k_y, 0) = 0.23 \frac{n^2 k^2}{(c_{11} k^2 + \alpha_L)^2} \frac{1}{2} \sum_i \vec{P}_i^2. \quad (5.2)$$

Here we have neglected the term k^2/k_ψ^2 . This is consistent, since the above model is restricted to low inductions, namely, to $b \ll 1$ for core interactions ($\xi \ll d$), and to $b \ll 1/2\kappa^2$ for magnetic interaction ($\lambda \ll d$).

Equation (5.2) could have been obtained also by a *classical* local theory, since it contains neither k_h nor k_ψ . The absence of k_h is, however, caused by the cancellation of two factors $(1 + k^2/k_h^2)^2$ in the denominator (magnetic nonlocality) and in the numerator (elastic nonlocality). This factor may become very large, $\approx b^2 \kappa^4$, at large values of κ . The physical reason for the appearance of the same k dependence in both the magnetic and the elastic nonlocalities is that at low inductions the flux lines interact only by the long-ranging magnetic field (except if κ is close to 0.7). On the other hand, at high inductions the elastic response becomes "more nonlocal" than the relationship between flux line positions and magnetic field. This is reflected in the appearance of the factor $1 + k^2/k_\psi^2$ in (3.3) and (4.2).

As a second example we consider pinning forces that derive from a potential $V(\vec{r})$. The force densities exerted by an inhomogeneity situated at $\vec{r} = \vec{a}$ then read

$$\vec{P}_\nu(z) = -\nabla_{\vec{r}_\nu} V(\vec{r}_\nu(z) - \vec{a}) = \nabla_{\vec{a}} V(\vec{r}_\nu(z) - \vec{a}). \quad (5.3)$$

The gradients in (5.3) are defined as having no z component. If the flux lines form a regular lattice, one has

$$\vec{P}_\nu(z) = - \int \frac{d^3k}{8\pi^3} i\vec{k} \vec{V}(\vec{k}) e^{i\vec{k} \cdot (\vec{R}_\nu - \vec{a})}, \quad (5.4)$$

$$\vec{P}(\vec{k}) = -n \sum_{\vec{K}} i(\vec{k}_2 + \vec{K}) \vec{V}(\vec{k} + \vec{K}) e^{-i\vec{a} \cdot (\vec{k} + \vec{K})}. \quad (5.5)$$

In (5.5) the sum is over all reciprocal-lattice vectors \vec{K} , and $\vec{k}_2 = (k_x, k_y, 0)$. The Fourier trans-

forms $\tilde{V}(\vec{k})$ and $\tilde{P}(\vec{k})$ of the continuous and discrete functions $V(\vec{r})$ and $\tilde{P}_v(z)$ are defined by (2.2) and (2.3), respectively. From (5.5) we obtain the average over \vec{a} :

$$\langle |\vec{k} \cdot \tilde{P}(\vec{k})|^2 \rangle = n^2 \sum_{\vec{K}} (k_z^2 + \vec{k}_2 \cdot \vec{K})^2 |\tilde{V}(\vec{k} + \vec{K})|^2. \quad (5.6)$$

Inserting this in (4.3) and using the rotational symmetry of $V(\vec{r})$ and $\tilde{V}(\vec{k})$ about the z axis and the relationship $k^2 \ll K_{10}^2$, we get the scattering intensity

$$I(k_x, k_y, 0) = 0.23 N \frac{n^4 (1 + k^2/k_\psi^2)^2 k^2}{(c_{11} k^2 + \alpha_L)^2} \times \left[k^2 |\tilde{V}(\vec{k})|^2 + \frac{1}{2} \sum_{\vec{K} \neq 0} K^2 |\tilde{V}(\vec{K})|^2 \right]. \quad (5.7)$$

For short-range forces (range $\ll d$) $\tilde{V}(\vec{k})$ is slowly varying. The sum in (5.6) may thus be transformed into an integral over $\vec{k}' = \vec{k} + \vec{K}$ with the integrand replaced by $k'^2 |\tilde{V}(\vec{k}')|^2 = |\tilde{P}(\vec{k}')|^2$, since $|\tilde{V}(\vec{k})|^2$ is even. Going back to real space and introducing $\tilde{P}(\vec{r}) = -\nabla V(\vec{r})$ (the gradient is still defined without z component), we get for the quantity in brackets in (5.7)

$$\frac{\pi}{n} \int_0^\infty dr r \tilde{P}(\vec{r})^2, \quad (5.8)$$

which does not depend on k . If the core width γ_0 enters the potential $V(\vec{r})$ only in the combination r/γ_0 , the integral (5.8) does not depend on γ_0 . For the model potential $V(\vec{r}) = \epsilon(1 + r^2/\gamma_0^2)^{-1}$, Eq. (5.8) becomes $\pi\epsilon^2/3n$. This model potential approximately applies to pinning centers interacting with the vortex core, the constant $|\epsilon|$ being of the order of $\mu_0 H_c^2 \xi^3$ or smaller.

The short-range case applies also to magnetic forces if $b \ll 1/2k^2$. At larger inductions magnetic forces have the long range $k_h^{-1} \gg d$. For long-range forces $\tilde{V}(\vec{k})$ decreases rapidly, in particular one has $|\tilde{V}(0)| \gg |\tilde{V}(\vec{K}_{10})|$ and thus the first term in the brackets of (5.7) becomes important. This term is strongly k dependent. The second term is independent of k and approximately equals (5.8). Magnetic interactions have an approximate potential³² $\tilde{V}(\vec{k}) = c(k_h^2 + k^2)^{-1}$ with $c = \vec{\mu} \cdot \vec{z} k_h^2 \phi_0 / \mu_0$ for magnetic inclusions with magnetic moment $\vec{\mu}$, and $c = \chi_0 k_h^2 B \phi_0 / \mu_0^2$ for para- or diamagnetic inclusions with strength χ_0 , or for crystal-lattice strains that couple to the magnetic energy density,^{33,34} [the perturbation energy is in these cases $F_1 = \vec{\mu} \cdot \vec{H}(\vec{a})$ and $F_1 = \frac{1}{2} \chi_0 H^2(\vec{a})$]. This potential gives for the quantity in brackets in (5.7)

$$c_2 [k^2 / (k_h^2 + k^2)^2 + c' / k_B^2], \quad (5.9)$$

where c' is close to unity for $b > 0.2$ and $c' \approx -\frac{1}{2} \ln b$ for $b < 0.2$.

The term $k^2 |\tilde{V}(\vec{k})|^2$ in (5.7) is due to the simultaneous action of one pinning center on many flux lines which leads to a change in the local flux density around the pinning center. The contribution of this term becomes large as the range of the pinning forces exceeds the flux line spacing. For short-range forces this term gives a small contribution.

Approximating the potential by $\tilde{V}(\vec{k}) = c(k_p^2 + k^2)^{-1}$, where $k_p = k_h$ for magnetic interaction and $k_p = \sqrt{2}/\xi$ for core interaction, we get in the general case of long- or short-ranging pinning forces deriving from a potential

$$I(k_x, k_y, 0) = 0.23 N \frac{n^4 c^2}{c_{11}^2 k_\psi^4} \left(\frac{k_\psi^2 + k^2}{k_\alpha^2 + k^2} \right)^2 \times \left(\frac{k^4}{(k_p^2 + k^2)^2} + c' \frac{k^2}{k_B^2} \right), \quad (5.10)$$

where $k_\alpha^2 = \alpha_L / c_{11}$, c and k_p^{-1} are the amplitude and the range of the potential, and $c' \approx 1$.

VI. PINNING FORCES DERIVED FROM GINZBURG-LANDAU THEORY

A more rigorous treatment of the pinning problem starts from the perturbed GL free-energy functional $F = F_0 + F_1$, where $F_0\{\Psi, \vec{A}\}$ is the free-energy functional of the homogeneous material (to which the material parameters H_c , H_{c2} , κ , λ , and ξ refer), and

$$F_1\{\Psi, \vec{A}\} = \int d^3r [-\alpha(\vec{r}) |\Psi|^2 + \frac{1}{2} \beta(\vec{r}) |\Psi|^4 + \gamma(\vec{r}) |(\nabla / i\kappa - \vec{A})\Psi|^2 + \vec{\mu}(\vec{r}) \cdot \vec{H} + \frac{1}{2} \chi(\vec{r}) H^2] \quad (6.1)$$

contains small perturbations α , β , γ , μ , and χ which are due to material inhomogeneities. The magnetic inhomogeneities are characterized by the functions $\vec{\mu}(\vec{r})$ and $\chi(\vec{r})$, and lead to pinning forces of the potential type that is discussed in Sec. V. The core interaction, characterized by α , β , and γ , for $b \lesssim 0.3$ is of the short-range type treated in Sec. V. At larger inductions, however, the core interaction exhibits a different behavior. This will be discussed in the following for localized perturbations with diameter $\leq \xi$. For such inhomogeneities $\alpha(\vec{r}) \approx \alpha_0 \delta(\vec{r} - \vec{a})$, $\beta(\vec{r}) \approx \beta_0 \delta(\vec{r} - \vec{a})$, and $\gamma(\vec{r}) \approx \gamma_0 \delta(\vec{r} - \vec{a})$, where α_0 , β_0 , and γ_0 give the strength of the perturbation. The pinning forces on the undisplaced lattice may be obtained by a method developed in Ref. 22. This gives³⁵ $\tilde{P}(\vec{k}) = \tilde{P}_\alpha(\vec{k}) + \tilde{P}_\beta(\vec{k}) + \tilde{P}_\gamma(\vec{k})$, where

$$\tilde{\tilde{P}}_{\alpha}(\vec{k}) = -\alpha_0 \omega(\vec{a}) k_B^2 \sum_{\vec{K}} \frac{i(\vec{k}_2 + \vec{K})}{k_{\Psi}^2 + k^2} e^{-i(\vec{K} + \vec{k}) \cdot \vec{a}}, \quad (6.2)$$

$$\tilde{\tilde{P}}_{\beta}(\vec{k}) = \beta_0 \omega^2(\vec{a}) k_B^2 \sum_{\vec{K}} \frac{i(\vec{k}_2 + \vec{K})}{k_{\Psi}^2 + k^2} e^{-i(\vec{K} + \vec{k}) \cdot \vec{a}}, \quad (6.3)$$

$$\tilde{\tilde{P}}_{\gamma}(\vec{k}) = \gamma_0 b \sum_{\vec{K}} \left(\frac{k_{\Psi}^2 \nabla \omega + (\vec{k}_2 + \vec{K})[(\vec{k} + \vec{K}) \cdot \nabla \omega]}{k_h^2 + (\vec{k} + \vec{K})^2} + \frac{(\nabla \omega)^2}{k_{\Psi}^2 + (\vec{k} + \vec{K})^2} + \frac{i(\vec{k}_2 + \vec{K}) \cdot \nabla \omega}{\omega} \right) e^{-i(\vec{K} + \vec{k}) \cdot \vec{a}}, \quad (6.4)$$

and $\omega = \omega(\vec{a}) = |\Psi(\vec{a})|^2$ is the value of the unperturbed periodic order parameter at the position of the defect. Equations (6.2) – (6.4) are exact in the limit $b \rightarrow 1$, and they remain good approximations in the entire range $0 < b < 1$. For $b > 0.5$, where ω is close to Abrikosov's solution, and for $k < 0.7 k_B$, where $(\vec{k} + \vec{K})^2 \approx \vec{K}^2$ for $\vec{K} \neq 0$, the relation

$$k_B^2 \sum_{\vec{K} \neq 0} \frac{-i\vec{K}}{K^2} e^{i\vec{K} \cdot \vec{r}} = \frac{\nabla \omega(\vec{r})}{\omega(\vec{r})} \quad (6.5)$$

may be used to simplify Eqs. (6.2) – (6.4):

$$\tilde{\tilde{P}}_{\alpha}(\vec{k}) = -\alpha_0 \left(\omega(\vec{a}) \frac{i\vec{k}_2 k_B^2}{k_{\Psi}^2 + k^2} + \nabla \omega(\vec{a}) \right) e^{-i\vec{k} \cdot \vec{a}}, \quad (6.6)$$

$$\tilde{\tilde{P}}_{\beta}(\vec{k}) = \beta_0 \left(\omega^2(\vec{a}) \frac{i\vec{k}_2 k_B^2}{k_{\Psi}^2 + k^2} + \nabla[\omega^2(\vec{a})] \right) e^{-i\vec{k} \cdot \vec{a}}, \quad (6.7)$$

$$\begin{aligned} \tilde{\tilde{P}}_{\gamma}(\vec{k}) = \gamma_0 \left[k_B^2 f_g(\vec{a}) \frac{i\vec{k}_2}{k_{\Psi}^2 + k^2} + \nabla f_g(\vec{a}) \right. \\ \left. + b[\nabla \omega(\vec{a}) \vec{k}] \vec{k}_2 \left(\frac{1}{-k_{\Psi}^2 + k^2} + \frac{1}{k_h^2 + k^2} \right) \right] \\ \times e^{-i\vec{k} \cdot \vec{a}}. \end{aligned} \quad (6.8)$$

In (6.8),

$$f_g(\vec{a}) = [\nabla \omega(\vec{a})]^2 / 2\kappa^2 \omega(\vec{a})$$

is the gradient term of the GL functional F_0 .³⁶ Note that $\nabla \omega$ and $\nabla(\omega^2)$ are odd functions of \vec{a} , whereas ω , ω^2 , and f_g are even. This greatly simplifies the averaging of $|\vec{k} \cdot \tilde{\tilde{P}}|^2$ over \vec{a} since the averaged product of an even and an odd function vanishes. The term $\tilde{\tilde{P}}_{\beta}$ may be neglected at sufficiently large b , since it is quadratic in $1 - b$, whereas $\tilde{\tilde{P}}_{\alpha}$ and $\tilde{\tilde{P}}_{\gamma}$ are linear in $1 - b$. The remaining terms can be evaluated analytically; we find in Appendix A:

$$\begin{aligned} \langle |\vec{k} \cdot \tilde{\tilde{P}}_{\alpha}(\vec{k})|^2 \rangle &= \alpha_0^2 \left(\langle \omega^2 \rangle \frac{k^2 k_B^2}{(k_{\Psi}^2 + k^2)^2} + \langle (\nabla \omega)^2 \rangle \frac{k^2}{2} \right) \\ &= \alpha_0^2 \langle \omega \rangle^2 \beta_A k_B^2 k^2 \left(\frac{k^2 k_B^2}{(k_{\Psi}^2 + k^2)^2} + \frac{1}{4} \right), \end{aligned} \quad (6.9)$$

$$\langle |\vec{k} \cdot \tilde{\tilde{P}}_{\gamma}(\vec{k})|^2 \rangle = \gamma_0'^2 k_B^2 \langle \omega \rangle^2 \frac{k^2}{4} \left[4a_1 \frac{k^2 k_B^2}{(k_{\Psi}^2 + k^2)^2} + a_2 + 2a_3 \left(\frac{k^2}{k_{\Psi}^2 + k^2} + \frac{k^2}{k_h^2 + k^2} \right) + \beta_A \left(\frac{k^2}{k_{\Psi}^2 + k^2} + \frac{k^2}{k_h^2 + k^2} \right)^2 \right], \quad (6.10)$$

$$2\langle \vec{k} \cdot \tilde{\tilde{P}}_{\alpha}(\vec{k}) \vec{k} \cdot \tilde{\tilde{P}}_{\gamma}(\vec{k}) \rangle = -\alpha_0 \gamma_0' k_B^2 \langle \omega \rangle^2 \frac{k^2}{2} \left[2\beta_A \frac{k^2 k_B^2}{(k_{\Psi}^2 + k^2)^2} + a_3 + \beta_A \left(\frac{k^2}{k_{\Psi}^2 + k^2} + \frac{k^2}{k_h^2 + k^2} \right) \right], \quad (6.11)$$

where $\gamma_0' = b\gamma_0$ and the constants $\beta_A = 1.1596$, $a_1 = 1.1125$, $a_2 = 8.2440$, and $a_3 = -3.0657$ are defined by the spatial averages $\langle \omega^2 \rangle = \langle \omega \rangle^2 \beta_A$, $\langle (\nabla \omega)^2 \rangle = b\kappa^2 \langle \omega \rangle^2 \beta_A$, $\langle f_g^2 \rangle = b^2 \langle \omega \rangle^2 a_1$, $\langle (\nabla f_g)^2 \rangle = b^3 \kappa^2 \langle \omega \rangle^2 a_2$ and $\langle \nabla \omega \nabla f_g \rangle$

$= b^2 \kappa^2 \langle \omega \rangle^2 a_3$.

Adding (6.9)–(6.11), we get

$$\langle |\vec{k} \cdot \tilde{\tilde{P}}(k_x, k_y, 0)|^2 \rangle = \langle \omega \rangle^2 k_B^2 k^2 \left[c_1 \frac{k^2 k_B^2}{(k_{\Psi}^2 + k^2)^2} + c_2 + c_3 \left(\frac{k^2}{k_{\Psi}^2 + k^2} + \frac{k^2}{k_h^2 + k^2} \right) + c_4 \left(\frac{k^2}{k_{\Psi}^2 + k^2} + \frac{k^2}{k_h^2 + k^2} \right)^2 \right], \quad (6.12)$$

where

$$c_1 = \beta_A \alpha_0^2 - \beta_A \alpha_0 \gamma_0' + a_1 \gamma_0'^2 = 1.160 \alpha_0^2 + 1.113 \gamma_0'^2 - 1.160 \alpha_0 \gamma_0' > 0,$$

$$c_2 = \frac{1}{4}(\beta_A \alpha_0^2 - 2a_3 \alpha_0 \gamma_0' + a_2 \gamma_0'^2) = 0.290 \alpha_0^2 + 2.061 \gamma_0'^2 + 1.533 \alpha_0 \gamma_0' > 0,$$

$$c_3 = \frac{1}{2}(-\beta_A \alpha_0 \gamma_0' + a_3 \gamma_0'^2) = -1.533 \gamma_0'^2 - 0.580 \alpha_0 \gamma_0' \geq 0,$$

$$c_4 = \frac{1}{4} \beta_A \gamma_0'^2 = 0.290 \gamma_0'^2 > 0.$$

With (6.12) inserted, the differential scattering cross section for $b > 0.5$ (4.2) becomes

$$I(k_x, k_y, 0) = 0.23N \frac{n^2}{c_{11}^2} \left(\frac{2bk^2}{2\kappa^2\beta_A - \beta_A + 1} \right)^2 \left(\frac{k_\psi^2 + k^2}{k_\alpha^2 + k^2} \right)^2 \frac{k^2}{k_B^2} \times \left[c_1 \frac{k^2 k_B^2}{(k_\psi^2 + k^2)^2} + c_2 + c_3 \left(\frac{k^2}{k_\psi^2 + k^2} + \frac{k^2}{k_h^2 + k^2} \right) + c_4 \left(\frac{k^2}{k_\psi^2 + k^2} + \frac{k^2}{k_h^2 + k^2} \right)^2 \right]. \quad (6.13)$$

In (6.12) the relationships (2.6)–(2.8) and $\langle \omega \rangle = 2\kappa^2(1-b)(2\kappa^2\beta_A - \beta_A + 1)^{-1}$ have been used.

VII. DISCUSSION

A. Intensity profile

The relationship between the differential scattering cross section for cold neutrons and the properties of the pinning centers are given by Eq. (5.2) for short-range forces, by (5.10) for potential forces, and by (6.12) for nonmagnetic pinning centers at $b > 0.5$. All three results apply to the case where the incident beam is parallel to the applied magnetic field, and where $k < 0.7k_B$ ($=0.37K_{10}$ for the triangular lattice). We first discuss the k dependence of the scattering intensity.

At very small $k \ll k_\alpha = (\alpha_L/c_{11})^{1/2}$, all three expressions yield $I(k) \sim k^{-2}$, with the constant of proportionality itself being proportional to the square of the ratio of pinning strength (P_i , c , α_0 , β_0 , γ_0) to Labusch's parameter α_L . Since α_L is roughly quadratic in the pinning strength, the scattering intensity is predicted to be inversely proportional to the strength of the pinning forces. This effect is probably difficult to observe because of masking by the primary beam. In principle, α_L may be determined from the position of the maximum in the differential scattering cross section at $k = k_\alpha$ (Fig. 3).

At $k \gg k_\alpha$, $I(k) \sim k^{-2}$ for short-range forces and for the GL result (6.13). For short-range forces, this decrease continues up to the BZ boundary, but for core interaction at $b > 0.5$, $I(\vec{k})$ reaches a constant value at $k \approx k_B(1-b)/b$. For long-range magnetic interaction $I(\vec{k}) \sim k^{-4}$ for $k_h < k < k_\psi$, and it reaches a constant value at $k \approx k_B[(1-b)/b]^{1/2}$,

$$I(k_x, k_y, 0) = 0.23Nn^2(\chi_0/\mu_0)^2 \times (B^2/\mu_0 c_{11})^2 (1/4\kappa^4). \quad (7.1)$$

The saturation value derived from (6.13) is

$$I(k_x, k_y, 0) = [0.20Nn^2 b^2 / (1 - 0.069\kappa^{-2})^2 c_{11}^2] \times (\alpha_0^2 - \alpha_0\gamma_0 b + 0.96\gamma_0^2 b^2), \quad (7.2)$$

where $0.20 = \gamma_n^2/16\beta_A$. For the special case $\gamma_0 = 0$, one has $c_3 = c_4 = 0$; the scattering cross section is then independent of k_h and, for $k > k_\alpha$, reduces to

$$I(k_x, k_y, 0) = \frac{0.20N\alpha_0^2 n^2 b^2}{(1 - 0.069\kappa^{-2})^2 c_{11}^2} \left[1 + \frac{1}{4} \left(\frac{k_\psi^2 + k^2}{kk_B} \right)^2 \right] \quad (7.3)$$

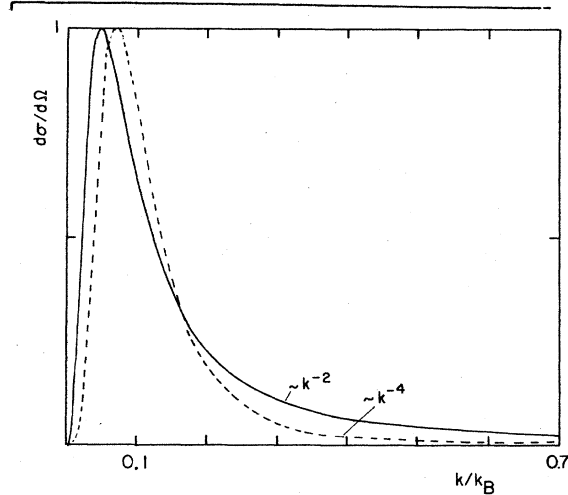


FIG. 3. Differential scattering cross section at low inductions ($b \leq 0.4$), Eq. (5.10), plotted for $k_\alpha = 0.05k_B$ and normalized to its maximum value. Solid line: Core interaction with range $k_p = 0.7\xi$ ($k_p^2 \gg k_B^2$). Dashed line: Magnetic interaction with range $k_p^{-1} = k_h^{-1} = \lambda(1-b)^{-1/2}$, plotted for $k_h = 0.1k_B$ corresponding to $b\kappa^2 = 50(1-b)$.

with (2.6) and (2.8) the last factor in (7.3) may be written

$$\left\{ 1 + \frac{1}{4} [(1-b)/bk' + k']^2 \right\}, \quad (7.3a)$$

where $k' = k/k_B$. For $b \gg 1/2\kappa^2$, where $c_{11} \sim b^2$, (7.3a) contains the entire b and k dependence of (7.3). The function (7.3a) is plotted in Fig. 4 for various values of b . The transition to the short-range-force behavior $I(\vec{k}) \propto k^{-2}$ is clearly seen at $b \leq 0.5$.

The first term, unity, in the brackets in (7.3) is due to the nonlocal elastic response of the FLL, leading to the factor k^4/k_ψ^4 in (4.2) which compensates the b dependence $(1-b)^2$ of the factor $\langle \omega \rangle^2$ originating from the pinning forces. This results in a large b - and k -independent contribution to $I(\vec{k})$ at large values of b and \vec{k} . Because of the approximations made, we cannot decide at present whether the increase of $I(\vec{k})$ continues up the BZ boundary. A maximum at the BZ boundary would be suggested by computations of the FLL strains caused by planar pinning forces,²⁶ which lead to pronounced oscillations with wave vectors $\frac{1}{2}\vec{K}_{10}$ and $\frac{1}{3}\vec{K}_{11}$. In addition to the pinning-force distribution and the elastic behavior of the FLL, which are known in principle, a calculation of the neutron scattering intensity

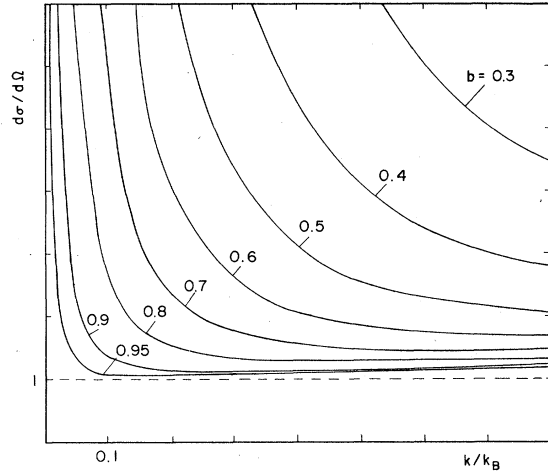


FIG. 4. Differential scattering cross section at high inductions ($b \gtrsim 0.6$), Eq. (7.3). Plotted is the expression (7.3a) for various values of b . This expression reproduces also the results at lower inductions if the pinning strength α_0 is interpreted as an adjustable parameter.

requires also the relationship between the displacement field and the magnetic field, which has not yet been calculated from GL theory for k close to the BZ boundary.

B. Total scattering cross section

The measured scattering cross section is an integral of $I(\vec{k})$ over some solid angle or an equivalent range of k_x and k_y . If the cross sections of the neutron beam and the detector are circular and concentric, the integral is over $k = (k_x^2 + k_y^2)^{1/2}$. For a well-collimated neutron beam and an annular detector (or an x - y -sensitive detector with appropriate circuitry) with minimum and maximum scattering angles $\theta_1 = k_1/k_n$ and $\theta_2 = k_2/k_n$, the total scattering cross section becomes

$$\sigma = \int d^2\Omega I(\vec{k}) = \frac{2\pi}{k_n^2} \int_{k_1}^{k_2} I(\vec{k}) k dk. \quad (7.4)$$

Figure 5 shows σ vs b for the special case (7.3). Also shown is that part of σ originating from the term $\sim k^{-2}$ in (7.3) that would follow from a local theory. This local term dominates at $b < 0.4$, but gives a negligible contribution at $b > 0.7$.

Introducing a dimensionless constant A , we may write

$$\sigma = N k_n^{-2} A, \quad (7.5)$$

and the probability for an incident neutron to be scattered into the detector becomes $p = L n_p k_n^{-2} A$, where L is the thickness of the specimen and $n_p = N/V$ is the density of pinning centers. For short-range forces Eq. (5.2) gives

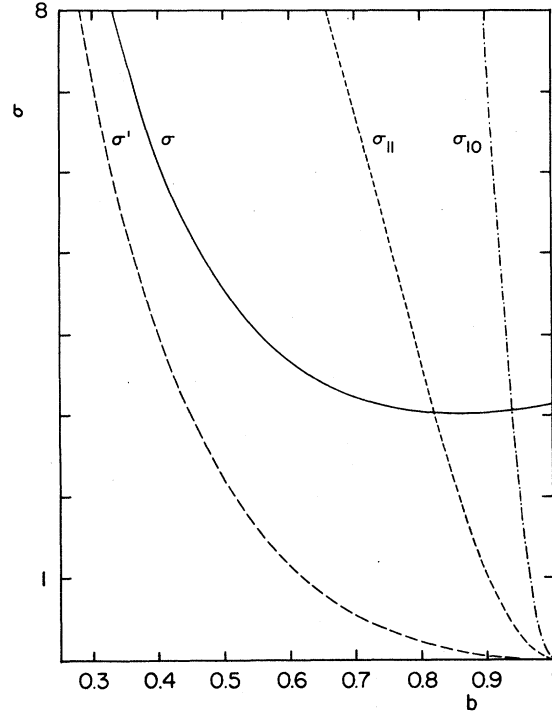


FIG. 5. Total scattering cross section σ for the case depicted in Fig. 4. Plotted is the expression (7.3a) integrated over $\xi^2 2\pi k dk$ from $0.255 k_B$ to $0.7 k_B$ (solid line). The dashed line gives the result that would follow from a theory neglecting all nonlocalities by omission of k^2 in the denominators of (2.5), (3.3), and (6.7). The dot-dashed line gives the total intensity (in the same units) of the six first Bragg reflections for the example discussed in the text below Eq. (7.14) and the dotted line gives the intensity of the six second-largest Bragg reflections at $t = 0.5$.

$$A = \frac{0.72 \ln(k_2/k_1) n^2}{c_{11}^2} \langle \vec{P}_i^2 \rangle. \quad (7.6)$$

The scattered intensity is thus proportional to the mean square of the pinning forces. This result, in contrast to the volume pinning force obtained from statistical summation theories, applies to arbitrarily weak pinning forces, and does not require a threshold force to be exceeded. A deviation from the simple result (7.6) occurs if the pinning forces are sufficiently strong to lead to considerable distortions of the FLL, which in turn lead to a weakening of the pinning forces, as discussed in Sec. IV.

We estimate the scattering probability for three simple examples. In all three cases we characterize the strength of the pinning sites by a dimensionless parameter ϵ with $|\epsilon| \lesssim 1$, and we use the approximation

$$c_{11} = B^2 \partial H_a / \partial B \approx \mu_0 H_c^2 b^2 (2\kappa^2 - 1).$$

For short-range forces with a potential $V(\vec{r})$

$= \epsilon \mu_0 H_c^2 \xi^3 (1 + r^2/r_0^2)^{-1}$, we get from (5.7) and (5.8) for $b < 0.3$

$$A = [0.0017 \ln(k_2/k_1) / (\kappa^2 - \frac{1}{2})^2 b] \epsilon^2. \quad (7.7)$$

For pinning centers with

$$(\alpha_0^2 - \alpha_0 \gamma_0 b + \gamma_0^2 b^2)^{1/2} = \epsilon \mu_0 H_c^2 \xi^3$$

we get from (7.2) for $b > 0.6$ and $k_2 = 0.7 k_B$

$$A = [0.016 (1 - k_2^2/k_1^2) / (\kappa^2 - \frac{1}{2})^2 b] \epsilon^2. \quad (7.8)$$

If we assume a neutron wavelength of $2\pi/k_n = 4 \times 10^{-10}$ m, a pinning density $n_p = 10^{21}$ m⁻³ corresponding to a mean separation of pinning centers of 10^{-7} m $= (\phi_0/2kG)^{1/2}$, a specimen thickness $L = 10^{-2}$ m, a range of scattering angles $\theta_2/\theta_1 = k_2/k_1 = 3$, a pinning strength $\epsilon = 0.4$, and $\kappa = 1.4$, we get for $b = 0.25$ from (7.8): $A = 0.0005$ and $p = 1.9 \times 10^{-5}$. If we correct for the fact that, for such small values of κ and b , the $c_{11} \approx B^2/\mu_0$ used in the derivation of (7.8) is too large by about a factor of 2, we get larger values: $A = 0.002$ and $p = 8 \times 10^{-5}$. With the same data, we get for $b = 0.8$ from (7.8): $A = 0.0011$ and $p = 5 \times 10^{-5}$. These results mean that for $b = 0.25$ (0.8) roughly one in every 13 000 (20 000) incident neutrons is scattered into the detector. This result, however, is rather sensitive to the values of κ , ϵ , and n_p chosen

For long-range magnetic forces ($b \gg 1/2\kappa^2$) we get from (5.7) and (5.9) for $k_2 = 0.7 k_B$

$$A = \frac{0.0181 b^3}{(\kappa^2 - \frac{1}{2})^2} [p^2 q^2 + (8p + 4p^2) \ln q + 1.25 + p] \epsilon^2, \quad (7.9)$$

where $p = (1 - b)/b$ and $q = k_2/\max(k_1, k_n) \geq 2$. For short-range magnetic forces ($b < \frac{1}{2}\kappa^2$), the bracket in (7.9) has to be replaced by $4(1 - b)^2 b^{-2} \ln(k_2/k_1)$. Using the same values as above ($\kappa = 1.4$, $k_2/k_1 = 3$, $\epsilon = 0.5$), we get for $b = 0.8$: $A = 0.0006$, and for $b = 0.25$: $A = 0.0013$ or $A = 0.005$ with the improved value of c_{11} .

C. Comparison with the intensity of Bragg reflections

The absolute value of the scattering probability can be measured by raising the applied field above H_{c2} . This procedure permits the intensity and profile of the incident beam and the background to be measured with the specimen in position. An alternative method is to measure the intensity of the Bragg reflections from the same imperfect specimen and relate it to the intensity inside the first BZ. We assume the integral intensity of the strongest Bragg reflections to be unchanged by the lattice distortions. An annular detector should be used to measure the first six reflections simultaneously. Such an arrangement measures

the integral over k_x and k_y of the intensity $I(\vec{k})$, depicted in Fig. 2, in the plane $k_z = 0$. If the sample is not rocked, the intensity in this plane depends on the degree of imperfection and on the exactness of the alignment of applied field and incident neutron beam. For an ideal FLL one has $I(\vec{k}) \sim \delta(k_z) = k_n^{-1} \delta(\phi)$, where ϕ is the alignment angle; thus $I(\vec{k})$ would be infinite for perfect alignment but zero for misalignment. The sensitivity to the alignment decreases with increasing lattice distortions, but then a comparison with theory is not possible since the theory of the intensity profile of the Bragg reflections from the imperfect FLL is still incomplete (Sec. I).

One therefore has to rock the sample to achieve integration over k_z . Rocking the sample together with the applied field by an angle $\pm \phi$ about the x axis corresponds to rocking of the toroidal intensity distribution of Fig. 2 about the k_x axis. The time-averaged intensity is now smeared out along k_z by the amount $\Delta k_z = 2\phi |k_y|$, which, averaged over a ring of radius K_{10} , gives $\langle \Delta k_z \rangle = 4\phi K_{10}/\pi$. The rocking width should be everywhere larger than the intrinsic width of the reflections which we expect to be comparable to k_B . Obviously this condition cannot be achieved for small values of $|k_y|/K_{10}$ by rocking about the x axis. The following expressions are thus only estimates. Inserting (2.4b) into (2.1) and using the relationship $8\pi^3 \delta(\vec{k} = 0) = V$, the sample volume, we get the differential scattering cross section for Bragg reflections

$$I(\vec{k}) = 0.23 V 8\pi^3 n^2 \sum_{\vec{K}} h_{mn}^2 \delta(\vec{k} - \vec{K}), \quad (7.10)$$

where $h_{mn} = \mu_0 H_{mn}/B$ are the form factors of the field. An annular detector (det), summing over the first six reflections, measures a total scattering cross section

$$\begin{aligned} \sigma_{10} &= k_n^{-2} \int_{\text{det}} dk_x dk_y I(k_x, k_y, 0) \\ &= 0.23 V 8\pi^3 n^2 k_n^{-2} 6h_{10}^2 \delta(k_z), \end{aligned} \quad (7.11)$$

where H_{10} is the largest Fourier coefficient of $H(\vec{r})$ (Appendix B). In the time average, rocking the sample smears out the δ function over a range $\langle \Delta k_z \rangle$; thus $\delta(k_z)$ has to be replaced by $\langle \Delta k_z \rangle^{-1} = \pi/4\phi K_{10}$, and the Bragg scattering cross section becomes

$$\sigma_{10} = 0.23 V 8\pi^3 n^2 k_n^{-2} h_{10}^2 (3\pi/2\phi K_{10}). \quad (7.12)$$

Inserting in (7.12) the $h_{10} = (1 - b)/14.2b\kappa^2$ of Appendix B, and using $K_{10} = 8^{1/2}\pi 3^{-1/4}n^{1/2}$, we obtain

$$\alpha_{10} = (n^{3/2}/k_n^2)[(1-b)^2/b^2\kappa^4](0.20/\phi). \quad (7.13)$$

Comparing this with (7.5), we get the ratio of the two scattering cross sections [expressions (7.7) and (7.8) for A give the same estimate if $k_2/k_1 \approx 3$]:

$$\sigma/\sigma_{10} = n_p(\phi_0/B_{c2})^{3/2}b^{-1/2}(1-b)^{-2}\epsilon^2 0.08\phi. \quad (7.14)$$

For the example ($n_p = 10^{21} \text{ m}^{-3}$, $\epsilon = 0.4$, $B_{c2} = 3 \text{ kG}$, and $\phi = 0.5 \text{ rad}$), we get

$$\sigma/\sigma_{10} = 0.004 b^{-1/2}(1-b)^{-2}. \quad (7.15)$$

This estimate gives $\sigma/\sigma_{10} = 1$ (0.1, 0.013) for $b = 0.94$ (0.8, 0.25). As in the estimate of Sec. VII B, the value for $b = 0.25$ becomes larger, $\sigma/\sigma_{10} = 0.05$, if a more realistic, smaller c_{11} is used.

The Bragg-scattering cross section (7.13) is depicted in Fig. 5 for the above example in units that give the correct ratio (7.15) between the plotted curves. Also plotted is the intensity of the six second-largest Bragg reflections σ_{11} for reduced temperature $t = 0.5$, where $\sigma_{11}/\sigma_{10} = (h_{11}/h_{10})^2 = 0.014$. The GL result ($\sigma_{11}/\sigma_{10} = 0.0007$ at $t = 0$) is unrealistic in this case; σ_{11}/σ_{10} is expected to depend quite sensitively on t , b , and the lattice distortions.

VIII. SUMMARY

(i) The neutron scattering intensity from the imperfect FLL may be calculated in five independent steps: calculate (a) the pinning-force field for one pinning center, (b) the pinning-force field for many pinning centers using some statistics, (c) the elastic distortions of the FLL due to these forces, (d) the magnetic field of the distorted FLL, and (e) the differential neutron scattering intensity of this spatially varying field.

(ii) These separate problems have been solved in this paper within GL theory: step (a) for small flux-line displacements, (b) for statistically independent pinning sites and small flux-line displacements, i.e., for uncorrelated pinning forces, (c) for small strains in the FLL, (d) for small strains and wave vectors \vec{k} well inside the first BZ, and step (e) within the Born approximation.

(iii) Since step (d) has not yet been solved for \vec{k} close to the Bragg reflections, a rigorous interpretation of scattering experiments is possible only for small-angle scattering with \vec{k} inside the first BZ. At sufficiently large induction more neutrons will be scattered into the first BZ than into the Bragg reflections.

(iv) The intrinsic defects and all shear and tilt deformations of the FLL give no contribution to the scattered intensity if the incident neutron beam is directed parallel to the applied magnetic

field. Only the elastic constant c_{11} enters the final result. It follows from Eq. (3.7) that this requires alignment of the two axes within an angle $(c_{66}/c_{44})^{1/2} \approx (1-b)/3b^{1/2}\kappa$.

(v) The small-angle scattering intensity is proportional to the sum of the squares of all pinning forces (for $b < 0.5$) or of all pinning strengths (for $b > 0.5$). In contrast to theories of the volume pinning force, this proportionality applies to arbitrarily weak pinning and does not exhibit a threshold.

(vi) At large inductions the differential scattering cross section $d\sigma/d\Omega$ depends only weakly on \vec{k} . This is in contrast to the result of usual *local* theories that assume the pinning forces to be short ranged and the elastic response of the FLL to be local. Such a theory would yield $d\sigma/d\Omega \sim k^{-2}$ in the entire BZ.

(vii) Within the present theory the scattering cross section attains a constant value at B_{c2} in contrast to the Bragg reflections which vanish as $(B_{c2} - B)^2$. This effect is due to the strong non-local elastic response of the FLL and applies to sufficiently weak pinning. In reality, σ will decrease below the weak-pinning result close to B_{c2} and vanish at B_{c2} due to flux line trapping or *synchronization* by the pinning centers, which leads to a breakdown of the assumption made in step (b).

ACKNOWLEDGMENT

This work was supported by the U. S. Department of Energy, Office of Basic Energy Sciences, Materials Sciences Division, and by the Deutsche Forschungsgemeinschaft. The author expresses his gratitude to J. R. Clem for his hospitality and for stimulating discussion and to D. K. Christen, P. Thorel, and J. Schelten for valuable advice.

APPENDIX A: EVALUATION OF THE AVERAGES IN SEC. IV

The evaluation of the spatial average

$$\langle |\vec{k} \cdot \vec{\tilde{P}}(\vec{k})|^2 \rangle \approx \langle |\vec{k} \cdot \vec{\tilde{P}}_\alpha(\vec{k}) + \vec{k} \cdot \vec{\tilde{P}}_\gamma(\vec{k})|^2 \rangle,$$

with $\vec{\tilde{P}}_\alpha(\vec{k})$ and $\vec{\tilde{P}}_\gamma(\vec{k})$ defined by (6.6) and (6.8) is straightforward by expressing ω , $\nabla\omega$, f_g , and ∇f_g as Fourier series. For the Abrikosov solution and the triangular lattice one has

$$\omega(\vec{r}) = \sum_{\vec{k}} \omega_{\vec{k}} e^{i\vec{k} \cdot \vec{r}},$$

$$\nabla\omega(\vec{r}) = \sum_{\vec{k}} \omega_{\vec{k}} i\vec{k} e^{i\vec{k} \cdot \vec{r}},$$

$$\omega_{\vec{k}} = \langle \omega \rangle (-)^{\nu^2} e^{-\nu^2 \pi / \sqrt{3}},$$

$\nu^2 = K_{mn}^2/K_{10}^2 = m^2 + mn + n^2 = 1, 3, 4, 7, 7, 9, \dots$, where m and n are the indices of the reciprocal-lattice vectors $\vec{K} = \vec{K}_{mn}$. In order to get the Fourier series for f_g , we take advantage of Eq. (6.5), which applies to any solution of the linearized first GL equation. We get (with $k_B^2 = 2b\kappa^2$)

$$\begin{aligned} \nabla \frac{\nabla \omega(\vec{r})}{2b\kappa^2 \omega(\vec{r})} &= \nabla \sum_{\vec{K} \neq 0} \frac{-i\vec{K}}{K^2} e^{i\vec{K} \cdot \vec{r}} \\ &= \sum_{\vec{K}} e^{i\vec{K} \cdot \vec{r}} - 1 = \frac{1}{n} \sum_{\vec{R}} \delta(\vec{r} - \vec{R}) - 1. \end{aligned}$$

If we exclude the singular points $\vec{r} = \vec{R}_\nu$, the periodic flux line positions, we get

$$\nabla \frac{\nabla \omega(\vec{r})}{\omega(\vec{r})} = -2b\kappa^2 = -\frac{(\nabla \omega)^2}{\omega^2} + \frac{\nabla^2 \omega}{\omega}, \quad (\text{A1})$$

and thus

$$f_g = \frac{(\nabla \omega)^2}{2\kappa^2 \omega} = b\omega + \frac{\nabla^2 \omega}{2\kappa^2} = b \sum_{\vec{K}} \omega_{\vec{K}} \left(1 - \frac{K^2}{2b\kappa^2}\right) e^{i\vec{K} \cdot \vec{r}}.$$

Using the relationship $K^2 = 2b\kappa^2 2\pi/\sqrt{3}$, we get, with $a = 2\pi/\sqrt{3}$ and $A = e^{-a} = 0.0266$,

$$\langle \omega^2 \rangle = \langle \omega \rangle^2 \beta_A, \quad \beta_A = 6 \sum_{\nu} A^{\nu^2} = 1.1596,$$

$$\langle (\nabla \omega)^2 \rangle = \langle \omega \rangle^2 b\kappa^2 a_0, \quad a_0 = 12a \sum_{\nu} \nu^2 A^{\nu^2} = 1.1596,$$

$$\langle f_g^2 \rangle = \langle \omega \rangle^2 b^2 a_1,$$

$$a_1 = 6 \sum_{\nu} A^{\nu^2} (1 - a\nu^2)^2 = 1.1125;$$

$$\langle (\nabla f_g)^2 \rangle = \langle \omega \rangle^2 b^3 \kappa^2 a_2,$$

$$a_2 = 12a \sum_{\nu} \nu^2 A^{\nu^2} (1 - a\nu^2)^2 = 8.2440;$$

$$\langle (\nabla \omega)(\nabla f_g) \rangle = \langle \omega \rangle^2 b^2 \kappa^2 a_3,$$

$$a_3 = 12a \sum_{\nu} \nu^2 A^{\nu^2} (1 - a\nu^2) = -3.0657.$$

The sums converge very rapidly. Finally, we prove that $a_0 = \beta_A$. From (A1) we get

$$(\nabla \omega)^2 = 2b\kappa^2 \omega^2 + \omega \nabla^2 \omega$$

and

$$\langle (\nabla \omega)^2 \rangle = 2b\kappa^2 \langle \omega^2 \rangle + \langle \nabla(\omega \nabla \omega) \rangle - \langle (\nabla \omega)^2 \rangle.$$

The average of the gradient of a periodic function vanishes and thus $\langle (\nabla \omega)^2 \rangle = b\kappa^2 \langle \omega^2 \rangle$, or $a_0 = \beta_A$. This general relationship holds for any periodic solution of the linearized first GL equation.

APPENDIX B: FORM FACTORS OF THE IDEAL FLUX LINE LATTICE

The Fourier coefficients H_{mn} or form factors $h_{mn} = \mu_0 H_{mn}/B$ of the magnetic field of the ideal triangular FLL within the GL theory depend only on κ and b :

$$\begin{aligned} h_{mn} &= \frac{1}{1 + K_{mn}^2 \lambda^2 / \langle \omega \rangle} \\ &= \frac{\langle \omega \rangle 0.276}{\langle \omega \rangle 0.276 + 2b\kappa^2 (m^2 + mn + n^2)} \quad (b \ll 1), \quad (\text{B1}) \end{aligned}$$

$$\begin{aligned} h_{mn} &= \frac{\exp[-(\pi/\sqrt{3})(m^2 + mn + n^2)]}{2b\kappa^2} \\ &= \frac{(1-b)(-0.163)^{m^2 + mn + n^2}}{2b\kappa^2 1.16 - b0.16} \quad (1-b \ll 1). \quad (\text{B2}) \end{aligned}$$

Equation (B1) may be interpreted as originating from a generalized London model in which λ is replaced by $\lambda \langle \omega \rangle^{-1/2}$. For $K_{mn} > \xi^{-1}$, the form factors are smaller than (B1).^{22,37-39} Equation (B2) follows from the linearized GL theory.³⁹ Numerical calculations³⁹ show that the higher form factors ($m^2 + mn + n^2 > 1$) increase with decreasing b rather rapidly. In particular, all negative h_{mn} change sign at values of b that are close to unity. For the first form factor ($m^2 + mn + n^2 = 1$) (B2) has, however, a large range of validity, $b > 0.5$ or larger. A useful interpolation formula between (B2) and (B2) is

$$h_{10} = (1-b)/[1 + b(14.2\kappa^2 - 1.98)] \quad (0 < b < 1). \quad (\text{B3})$$

At reduced temperatures, $t = T/T_c < 1$, the form factors were derived from the Gorkov theory for $b \approx 1$ by Delrieu^{40,41} and for $0 < b < 1$ numerically by the author.⁴² These results show that (B3) remains a good approximation at $t < 1$, except for very clean superconductors at $t < 0.1$. The higher Fourier coefficients, however, increase rapidly as t decreases from unity. For example, for a clean superconductor at $b \approx 1$, one finds⁴³ $h_{11}/h_{10} = 0.232$ (0.219, 0.168, 0.117, 0.074, 0.039, 0.027) at $t = 0$ (0.1, 0.3, 0.5, 0.7, 0.9, 1). The increase of the ratio h_{11}/h_{10} , h_{20}/h_{10} , etc., as b or t decreases from unity, should be seen in neutron scattering experiments, since the scattering cross section of Bragg reflections is proportional to h_{mn}^2 .

- *On leave from Max-Planck-Institut für Metallforschung, Institut für Physik, Stuttgart, Germany.
- ¹D. Cribier, B. Jacrot, L. M. Rao, and B. Farnoux, *Phys. Lett.* **9**, 106 (1964).
 - ²J. Schelten, H. Ullmaier, and W. Schmatz, *Phys. Status Solidi B* **48**, 619 (1971).
 - ³Y. Simon and P. Thorel, *Phys. Lett.* **28**, 1370 (1971).
 - ⁴D. Cribier, Y. Simon, and P. Thorel, *Phys. Rev. Lett.* **28**, 1370 (1972).
 - ⁵P. Thorel, R. Kahn, Y. Simon, and D. Cribier, *J. Phys.* **34**, 447 (1973).
 - ⁶R. Kahn and G. Porette, *Solid State Commun.* **13**, 1839 (1973).
 - ⁷H. W. Weber, J. Schelten, and G. Lippmann, *Phys. Status Solidi B* **57**, 515 (1973).
 - ⁸G. Lippmann, J. Schelten, R. W. Hendricks, and W. Schmatz, *Phys. Status Solidi B* **58**, 633 (1973).
 - ⁹J. Schelten, G. Lippmann, and H. Ullmaier, *J. Low Temp. Phys.* **14**, 213 (1974).
 - ¹⁰M. Roger, R. Kahn, and J. M. Delrieu, *Phys. Lett.* **50A**, 291 (1974).
 - ¹¹J. Schelten, H. Ullmaier, and G. Lippmann, *Phys. Rev. B* **12**, 1772 (1975).
 - ¹²G. Lippmann, J. Schelten, and W. Schmatz, *Philos. Mag.* **33**, 475 (1976).
 - ¹³D. M. Kroeger and J. Schelten, *J. Low Temp. Phys.* **25**, 369 (1976).
 - ¹⁴D. K. Christen, F. Tasset, S. Spooner, and H. A. Mook, *Phys. Rev. B* **15**, 4506 (1977).
 - ¹⁵R. Labusch, *Phys. Status Solidi B* **69**, 539 (1975).
 - ¹⁶A. M. Campbell, and J. Evetts, *Critical Currents in Superconductors* (Taylor and Francis, London, 1972).
 - ¹⁷A. M. Campbell, in *International Discussion Meeting on Flux Pinning in Superconductors*, edited by P. Haasen and H. C. Freyhardt (Goltze, Göttingen, 1975).
 - ¹⁸E. J. Kramer, *J. Appl. Phys.* **49**, 742 (1978).
 - ¹⁹R. Schmucker and H. Kronmüller, *Phys. Status Solidi B* **61**, 181 (1974).
 - ²⁰E. H. Brandt, *J. Low Temp. Phys.* **26**, 709 (1977).
 - ²¹E. H. Brandt, *J. Low Temp. Phys.* **26**, 735 (1977).
 - ²²E. H. Brandt, *J. Low Temp. Phys.* **28**, 263 (1977).
 - ²³E. H. Brandt, *J. Low Temp. Phys.* **28**, 291 (1977).
 - ²⁴R. Schmucker and E. H. Brandt, *Phys. Status Solidi B* **79** (1977).
 - ²⁵E. H. Brandt, *Phys. Lett.* **61A**, 413 (1977).
 - ²⁶E. H. Brandt, *Phys. Status Solidi B* **84**, 269 (1977).
 - ²⁷E. H. Brandt, *Phys. Status Solidi B* **84**, 637 (1977).
 - ²⁸P. G. DeGennes, *Superconductivity of Metals and Alloys* (Benjamin, New York, 1966).
 - ²⁹R. Labusch, *Phys. Lett.* **22**, 9 (1966).
 - ³⁰R. Labusch, *Cryst. Latt. Defects* **1**, 1 (1969).
 - ³¹It should be noted that α_L is not linear in the pinning strength, although it is the spatial average over the curvature of the pinning potentials. Weak pinning forces yield $\alpha_L=0$ since they are uncorrelated. Both a finite α_L and a finite volume pinning force result only if the pinning forces are sufficiently large to be correlated by the elastic response of the FLL. It is only this correlation that leads to finite mean values of the second and first derivatives of the pinning potentials. For weak pinning we expect α_L to be proportional to the square of the pinning strength.
 - ³²E. H. Brandt, *Philos. Mag.* **37**, 293 (1978).
 - ³³A. Seeger and H. Kronmüller, *Phys. Status Solidi* **27**, 371 (1968).
 - ³⁴H. Kronmüller and A. Seeger, *Phys. Status Solidi* **34**, 781 (1969).
 - ³⁵E. H. Brandt (unpublished).
 - ³⁶At large b the two parts $(\nabla\omega)^2/4\kappa^2\omega$ and ωQ^2 of the gradient term $|(\nabla/i\kappa - A)\Psi|^2$ are identical. This gives rise to the factor of 2 (rather than of 4) in the denominator of f_g .
 - ³⁷J. R. Clem, *J. Low Temp. Phys.* **18**, 427 (1974).
 - ³⁸J. R. Clem, in *Low Temperature Physics, LT 14*, edited by M. Krusius and M. Vuorio (North-Holland, Amsterdam, 1975), Vol. 2, pp. 461-464.
 - ³⁹E. H. Brandt, *Phys. Status Solidi B* **51**, 345 (1972).
 - ⁴⁰J. M. Delrieu, *J. Low Temp. Phys.* **6**, 197 (1972).
 - ⁴¹J. M. Delrieu, thesis (Université Paris-Sud, 1974) (unpublished).
 - ⁴²E. H. Brandt, *Phys. Status Solidi B* **77**, 105 (1976).
 - ⁴³E. H. Brandt, *Phys. Lett.* **43A**, 539 (1973).